RASĀYAN *J. Chem.*
Vol. 19 | Special Issue | 174-186 | 2026
ISSN: 0974-1496 | e-ISSN: 0976-0083 | CODEN: RJCABP
http://www.rasayanjournal.com
http://www.rasayanjournal.co.in

SURFACE-FUNCTIONALIZED ACTIVATED CARBON DERIVED FROM PEANUT SHELL BIOMASS AS SUPERCAPACITOR ELECTRODES FOR ENERGY STORAGE

R. Sakthivel[1],R. Mohamed Arfayeen[1,✉],R. Aruna[2],and G. Tabassum Fathima[3]
[1]Department of Electronics, PSG College of Arts and Science,
Coimbatore-641014, (Tamil Nadu) India
[2]Department of Biochemistry, SRM Arts and Science College,
Kattankulathur-603203, (Tamil Nadu) India
[3]Department of Mathematics, St. Peter's Institute of Higher Education and Research,
Avadi, Chennai, (Tamil Nadu) India
✉Corresponding author: arfu16elec@gmail.com

ABSTRACT
Biomass-derived activated carbons have attracted considerable interest as sustainable and cost-effective electrode materials for energy storage devices, particularly supercapacitors. In this research, activated carbon was synthesized from peanut shell agro-waste through pyrolysis followed by a two-step acid–alkali activation process. The structural, optical, and surface chemical properties of the prepared carbon were evaluated using X-ray photoelectron spectroscopy (XPS), X-ray diffraction (XRD), Fourier Transform Infrared (FTIR) spectroscopy, and UV–Visible (UV–Vis) spectroscopy. Electrodes were fabricated using polyvinyl alcohol (PVA) as a binder, and their electrochemical performance was evaluated using cyclic voltammetry (CV). The UV–Visible absorption profile revealed bands attributable to π–π* and n–π* electronic transitions, suggesting the existence of conjugated carbon frameworks along with oxygen-based surface functionalities. XPS and FTIR analyses confirmed various surface functionalities, including hydroxyl, carbonyl, pyridinic/pyrrolic nitrogen, phosphate, and sulfur-containing groups. XRD patterns revealed predominantly amorphous carbon with short-range graphitic ordering. Cyclic voltammetry measurements displayed quasi-rectangular voltammograms with good electrochemical reversibility, suggesting effective electric double-layer capacitance with contributions from pseudocapacitive surface functionalities. The synergistic effect of heteroatom doping and partial graphitization of peanut shell-derived activated carbon offers low-cost, sustainable electrodes for high-performance supercapacitors, advancing clean energy storage, resource efficiency, biomass valorization, green chemistry and environmental sustainability.
Keywords: Peanut Shell Derived Activated Carbon, Supercapacitor, UV–Vis Spectroscopy, FTIR, XRD, XPS, Cyclic Voltammetry

RASĀYAN *J. Chem.*, Thematic Issue, 2026

INTRODUCTION

Energy storage technologies can play a critical role towards addressing the growing global need for sustainable and efficient energy system. Supercapacitors have attracted considerable research interest because they offer extended cycle stability, rapid charging and discharging capabilities and high power density compared with conventional battery technologies.[1,2] Supercapacitors verify a lot on the characteristics of the electrode materials such as surface area, pore image, and surface functional groups which affects the charge storage by the electric double-layer capacitance and pseudocapacitance.[3,4] Activated carbon is a common electrode material because it has a high surface area, adjustable porosity, and is chemically stable. Low-cost, eco-friendly alternatives that offer a renewable source of carbon with highly heteroatomic levels, activating biomass to create activated carriers have gained popularity over the past few years.[5,6] Agricultural wastes (coconut shells, peanut shells and others) can be transformed into porous carbon materials and some functional groups that can help in the interaction of the electrolytes, adsorption of ions and redox reactions.[7–9] An excellent and agriculturally abundant byproduct that can be valorized to activated carbon by pyrolysis and chemical activation is the shell of peanuts. These carbon may comprise heteroatomic functionality (O, N, P, S), short-range graphitic order and purity of the

http://doi.org/10.31788/RJC.2026.19510008
This work is licensed under a CC BY 4.0 license.

surface, which are favorable electrode in supercapacitors.[3,10] Although there has been comprehensive research on biomass-derived carbons, there has been no detailed correlation of structural, surface and electronic properties with electrochemical activity of peanut shell-derived carbon. In spite of the rising attention in biomass-derived activated carbon for supercapacitor applications, additional examination is required to relate its structural, surface chemical and electrochemical characteristics with its energy-storage presentation.[11] Hence, the current study aims to methodically describe the prepared activated carbon using FTIR, UV–Vis, XRD, XPS and cyclic voltammetry and assess its potential as a sustainable supercapacitor electrode. The study supports SDG 7 – Affordable and Clean Energy by contributing to the development of sustainable energy-storage materials and aligns with the Green Chemistry and Environmental Sustainability through the value-added utilization of biomass resources.

EXPERIMENTAL

Raw Material Collection and Preparation

Peanut shell used was collected locally at a farm, and this was first rinsed in distilled water to remove dust and other debris. After two hours of drying at 100 °C, the portion was crushed into 5 mm pieces. This particular type of sizing was selected to increase the surface area thereby making the pyrolysis stage reaction easier.

Pyrolysis

The broken shells were added to a sealed crucible and heated at 600 °C for 12 hours in vacuum electric furnace. After the heating cycle was finished and the samples had cooled down, the carbon that was produced was removed out of the furnace and used later.

Milling and Sieving

Pyrolyzed carbon was ball-milled over a period of 2 hours to decrease the particle size. Following milling, the powdered material was passed through a sieve to obtain particles smaller than 300 μm, ensuring a relatively uniform particle size suitable for subsequent chemical activation and characterization.

Chemical Activation

To undergo the activation process, the carbonized powder was initially reacted with 1 M sulphuric (H_2SO_4) to stir over a period of two hours to remove impurities and also to introduce functional groups on the surface. The second step entailed incubation during the next two hours in 1M potassium hydroxide (KOH) to develop the pore structure required. All steps were ended with the extensive process of washing with use of distilled water until a neutral pH was reached, which was then followed by two hours of oven-drying at 100 °C.

Electrode Fabrication for Supercapacitor Applications

Particle Size Refinement

Ball-milling was used to further refine the acid-alkali activated carbon. The resulting powder was sieved to obtain particles with a size of less than 106 μm and hence a high degree of fineness and uniformity.

Binder Preparation

A binder solution was made by mixing 1 g of Polyvinyl Alcohol (PVA) in 75 mL of pure water. This mix was left stirring at room temperature to allow a stable medium of the electrode slurry, which was left in place waiting until the PVA was completely incorporated, about 20 minutes.

Slurry Composition and Coating

30 g of the prepared activated carbon was put into this solution and stirred. This gave a homogenous distribution of the carbon particles between the binder matrix. Lastly, the electrode was deposited by coating the substrate with the resultant slurry and then letting the slurry dry properly according to the recommended methodology.[12-15]

Optical Characterization

A UV-3600Plus Series spectrophotometer (Model S/N: UV3600, A12015600584) was used to analyse the optical properties of the activated carbon. Measurement was done in reflectance mode in wavelength

range of 200-800 nm. On the day of data acquisition, controlled laboratory operations were performed in order to secure quality data acquisition using UVProbe software (v2.70, Normal Mode).

Instrumental Parameters

Each spectral recording was done at a medium scan rate with a 1 nm sampling interval and 5 nm slit width. The time constant was set to 0.2 s and the source of light transitioned at 310 nm. To measure the reflectance characteristics of the carbon samples in their original state so as to accurately capture them, all the data were taken as original values.

Fourier Transform Infrared (FTIR) Spectroscopy

The surface chemistry of the peanut shell-derived activated carbon was examined using FTIR spectroscopy to determine the functional groups associated with its surface. The FTIR spectra were acquired using an FTIR spectrometer over the wavenumber range of 4000–400 cm^{-1}. It was measured at 30 scans with a resolution of 4 cm^{-1} and Happ-Genzel apodization. The KBr pellet method of sample preparation was used.

The obtained spectra were compared to determine typical absorption bands, which refer to carbonyl (C=O), aliphatic (C–H), hydroxyl (O–H), and aromatic (C=C) functional groups. These outer characteristics are imperative in the interaction with electrolytes as well as in the pseudocapacitive conductivity, thus affecting the electrochemical conduct of activated carbon towards the use of supercapacitors.[1,2]

X-ray Diffraction (XRD) Analysis

XRD analysis was conducted to investigate the structural characteristics and phase composition of the activated carbon obtained from peanut shells. The powdered sample was analyzed using a powder diffractometer equipped with Cu Kα radiation, having wavelengths of λ_1 = 1.5406 Å and λ_2 = 1.54443 Å. Under continuous scan mode, patterns of diffraction were measured along the Gonio axis with a 2θ range of 5.01° to 99.98° C with a step time of 58.395 s and a step size of 0.022°C. Other instrumental parameters were a constant divergence slit in 0.9167°, a length of the specimen is 10 mm and measurements were done at a room temperature (25 °C). The generator was run at 40 kV and 15 mA. The diffraction patterns were measured to determine the extent of graphitization, the existing amorphous carbon, and any other crystallite phases. Bragg law was used to determine the crystallite size ($L_{(c)}$) and interlayer spacing (d-spacing) and relative peak intensities to determine the level of structural ordering. These structural features are intimately connected with the electrochemical performance of the material to be used in supercapacitor applications.[1,2]

X-ray Photoelectron Spectroscopy (XPS)

XPS spectroscopy was employed to characterize the surface elemental composition and chemical states of the peanut shell-derived activated carbon. The analysis was carried out using a monochromatic Al Kα X-ray source with a photon energy of 1486.6 eV (hν), operated at 24.3 W, with a beam spot diameter of 100 μm and a photoelectron take-off angle of 45°. Both survey scans and high-resolution spectra were acquired for the N 1s, C 1s, P 2p, O 1s, S 2p, and S u 1s regions. A pass energy of 55 eV was used for the C 1s, N 1s, O 1s, and P 2p spectra, whereas the S 2p spectrum was recorded at a pass energy of 280 eV. The obtained spectra were analysed to obtain binding energies, peak shifts, and atomic concentrations by standard peak deconvolution. Measurements were made with a range of 1.30 to 1.725 × 10^3 counts of intensity to provide trustworthy measurements of the surface functional groups. Such chemical characteristics of surfaces are strongly linked with electrochemical activity and charge-storage characteristics in supercapacitor usage.[1,2]

Electrochemical Evaluation

Cyclic voltammetry

To determine the charge storage mechanism and supercapacitive activity of the acid-alkali activated coconut shell carbon electrode, cyclic voltammetry (CV) was used to examine the behavior. You know, to maintain good electrical contact all electrode samples were mounted to a copper conductor and cold-mounted on a polyester base, furnishing both mechanical stability and keeping the conductor in place.

Measurements were conducted with the help of an ordinary three-electrode system. Electrochemical characterization was performed using a three-electrode cell, in which the prepared carbon material served as the working electrode. The three-electrode cell incorporated a platinum wire for current collection at the counter-electrode position, whereas the Ag/AgCl electrode provided the reference potential. The supporting electrolyte was 1 M H_2SO_4 solution. All data were measured using a Versa STAT 4 potentiostat. The experiments were carried out through cyclic voltammetry using a potential range of 0.05 V to 0.8 V in three sequential cycles at various scan rates of 20, 40, 60, 80 and 100 0.05 mV s^{-1}. The voltammograms obtained were used to interpret the electrochemical processes of the electrode material. The CV measurements were analyzed to determine key electrochemical charge-storage characteristics, including specific capacitance (Csp) and energy density (E), thereby assessing the suitability of the fabricated carbon electrode for supercapacitor applications.

RESULTS AND DISCUSSION

UV–Visible Spectroscopy

The UV–Visible (UV–Vis) absorption spectrum of activated carbon derived from peanut shells is shown in Table-1 and Fig.-1. Various absorption bands are evident in the spectrum as 200-800 nm which are attributed to electronic transitions within the carbonaceous framework. The UV–Vis spectrum confirms the presence of conjugated carbon networks through π–π* electronic transitions, along with oxygen-containing surface functional groups associated with n–π* transitions. The wide absorption tail at visible range is a sign of structural defects and amorphous regions, which is in agreement with the short-range graphitic ordering that is usually established in biomass-based carbon materials.[16,17] Heterogeneous surface functionalization is indicated by the absorption characteristics in the 300-500 nm area, which is beneficial to a high electrolyte wettability and charge-storage properties.[18,19] Particularly, the 301 nm band is attributed to π–π* transitions of sp^2-hybridized carbon domains, which are consistent with previous results on carbons obtained by the use of lignocellulosic materials.[18] The absorption peak at 217 nm is attributed to n–π* transitions of carbonyl and other oxygen functional groups useful in charge storage as a pseudocapacitive material.[16,17] Reflectance measurements, registered by UVProbe software (v 2.70, Normal Mode) can give insight into the electronic transitions of the surface. The transitions also unveil electronically active sites that are capable of enhancing adsorption of ion due to electrolyte and thus the specific capacitance and rate capacity of supercapacitor electrodes.[20,21] Generally, the UV-Vis analysis shows that the activated carbon of peanut shells consists of a mixture of graphitic domains and oxygen-functional groups, which plays a vital role in effective electrochemical energy storage, as was found when using biomass and poisons to produce carbons. UV–Visible spectrum of peanut shell-derived activated carbon showing π–π* and n–π* transitions from conjugated carbon networks and oxygen-containing functional groups that enhance supercapacitor performance.

Table-1: UV–Vis Peak Assignments of Peanut Shell-Derived Activated Carbon

Peak No.	Wavelength (nm)	Reflectance (%)	Interpretation
1	217	5.932	n–π* transition of carbonyl/oxygen groups, consistent with surface oxygen functionalities reported in biomass-derived carbons.[16,17]
2	301	6.924	π–π* transition in conjugated C=C systems, indicative of short-range graphitic domains.[18]
3	326	6.453	π–π* transition in aromatic clusters, as seen in lignocellulosic carbon materials.[19]
4	368–378	6.233–6.265	Oxygen-functionalized aromatic carbon, contributing to pseudocapacitance.[20]
5	400–432	6.043–5.937	Electron delocalization in aromatic clusters, enhancing electrical conductivity.[21]
6	440–508	6.006–5.755	Extended π conjugation and surface oxidation, promoting ion adsorption.[22]
7	563–579	5.676–5.800	Surface functional groups, relevant for electrolyte interaction.[16]

8	651–732	5.585–5.854	Long-range absorbance tail, indicative of defects and amorphous carbon regions.[17]
9	791	5.759	Low-energy transitions, suggesting extended conjugation.[18]

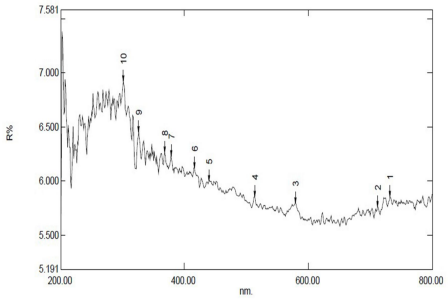


Fig.-1: UV–Visible Spectrum of Peanut Shell-Derived Activated Carbon.

FTIR Spectroscopy

The FTIR spectrum of peanut shell-derived activated carbon is shown in Fig.-2. The observed absorption features and their respective spectral assignments are provided in Table-2.

Table-2: FTIR Peak Assignments for Peanut Shell-Derived Activated Carbon

Peak (cm^{-1})	Intensity	Functional Group Assignment	Remarks / Relevance
445.56	45.41	C–H bending / skeletal vibrations	Minor contribution from aliphatic chains
476.42	45.74	C–H bending	Aliphatic structures from lignocellulose
493.78	46.85	C–H bending	Aromatic CH groups
586.36	44.80	C–O–C stretching	Ether linkage, surface functionalization
711.73	40.08	C–H bending (aromatic)	Aromatic ring structures
1097.50	35.31	C–O stretching	Alcohol or phenolic groups.[19]
1149.57	31.07	C–O–C stretching	Surface ether functionalities
1228.66	45.64	C–O stretching	Alcohol/phenolic groups
1359.82	49.92	C–H bending / CH_3 groups	Minor aliphatic residues
1448.54	45.24	C=C stretching (aromatic)	Conjugated carbon networks
1735.93	31.48	C=O stretching (carbonyl)	Oxygenated functional groups, important for pseudocapacitance.[22]
2210.42	66.76	C≡C stretching	Alkynes / triple bond structures
2341.58	57.67	O=C=O stretching	Carboxyl groups
2846.93	34.31	C–H stretching	Aliphatic chains
2912.51	29.99	C–H stretching	Methylene/methyl groups

3005.10	60.27	=C–H stretching	Aromatic or olefinic groups
3273.20	57.51	O–H stretching	Hydroxyl groups, enhances electrolyte interaction.[21]
3776.62	57.87	O–H stretching	Surface hydroxyls / phenolic groups
3984.93	56.93	–	Weak overtones or lattice vibrations

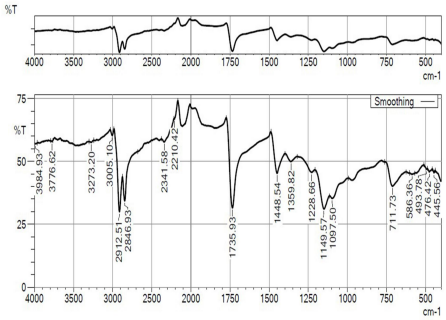


Fig.-2: FTIR Spectrum of Peanut Shell-Derived Activated Carbon.

Surface Chemical Environment

The FTIR profile confirms the presence of various oxygen-bearing functional groups and aromatic frameworks, aligning with established data for biomass-based carbons.[1,4] The detection of these oxygenated species is particularly significant as they improve the material's hydrophilicity. This, in turn, allows for better electrolyte accessibility within the pore network and introduces pseudocapacitive contributions to the overall energy storage mechanism.

Functional Group Impact

A high level of surface functionalization is contained in specific vibrations at 3273 cm^{-1} and 3776 cm^{-1}(O–H stretching), and a distinct peak at 1735 cm^{-1} (C=O stretching). The groups are the active sites of the adsorption of ions that is essential in terms of the maximum levels of charge storage.[5] Along with that, the aromatic C=C vibrations that are observed at around 1448 cm^{-1} position suggest the formation of graphitic domains in the carbon matrix. The structures are critical to the retention of electronic conductivity, which is required for the supercapacitor to perform at high rates. Altogether, the FTIR results show that both oxygen-functional groups and conjugated carbon networks are present in activated carbon produced by peanut shells, and these functional groups are beneficial in the electrochemical energy storage process. FTIR spectrum of activated carbon produced from peanut shells depicts typical absorption bands due to hydroxyl, carbonyl, ether, aliphatic, and aromatic populations that form the basis of pseudocapacitance and electrolyte interaction for use in supercapacitors.

XRD Analysis

The XRD pattern of the activated carbon prepared out of peanut shells exhibits a very high point at 2θ ≈ 26.43° and is associated with the (002) shell of graphitic carbon, realising the existence of short-range graphitic domains. Figure-3 presents the XRD pattern of the activated carbon prepared using peanut shells, and the major diffraction peaks along with details are presented in Table-3. These graphitic areas have enhanced the efficiency of the electrodes in a supercapacitor as they can transport electrons.[19,20] At lower angles (10–24° 2θ) broad diffraction which appears indicates the presence of amorphous carbon and disordered structures that result in high surface area that allows adsorption of ions.[21] Other peaks at 39–42° 2θ range correspond to in-plane ordering (100) and (101) planes, verifying some crystallinity, and biomass-based carrier carbon gives rise to these peaks. In general, the XRD findings are indicative of an amalgamation of graphitic and amorphous structures of the activated carbon, which would offer concurrently electronic conductivity and accessible surface area, which are desirable properties of high-performance supercapacitors electrodes. The X-ray diffraction pattern of the activated carbon of peanut

shells clearly shows a strong (002) peak that is typical of graphitic carbon and broader peaks indicating amorphous carbon and partially ordered structures. These properties mean that its structure is a mixture of both graphitic and disordered areas, including electron conduction and a large surface area which are suitable for use as a supercapacitor electrode.

Table-3: XRD Peak Positions, d-spacing, and Relative Intensities for Peanut Shell-Derived Activated Carbon

Peak No.	Height (cts)	2θ (°)	FWHM (°2θ)	Relative Intensity (%)	d-spacing (Å)	Assignment / Interpretation
1	119.54	10.28	0.866	49.84	8.603	Amorphous carbon / disordered domains
2	114.59	11.57	0.520	47.77	7.650	Amorphous regions / short-range ordering
3	121.67	14.62	0.520	50.72	6.060	Partial graphitic stacking
4	104.89	21.57	0.520	43.73	4.120	(002) plane, indicative of short-range graphitic order.[19]
5	77.26	24.11	0.693	32.21	3.691	Amorphous carbon contribution
6	239.85	26.43	0.520	100.00	3.372	(002) graphitic peak, primary graphitic stacking, responsible for electronic conductivity.[22]
7	86.20	39.74	0.693	35.94	2.268	(100) in-plane ordering of graphene layers
8	62.46	42.65	1.386	26.04	2.120	(101) planes, indicating partial crystallinity

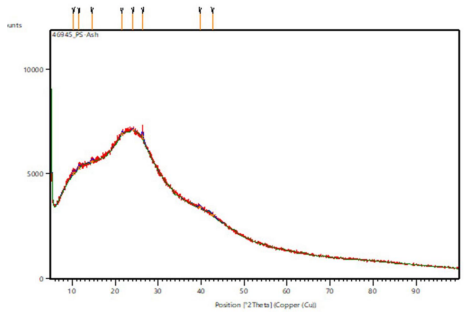


Fig.-3: X-Ray Diffraction (XRD) Pattern of Peanut Shell-Derived Activated Carbon

X-ray Photoelectron Spectroscopy (XPS)

Survey Spectrum

The XPS Survey Spectrum showed that there is nitrogen (N), carbon (C), phosphorus (P), oxygen (O), sulfur(S), and trace elements (Su) present on the surface of peanut shell activated carbon and the atomic percentages are presented in Table-4 and Fig.-4 to Fig.-9. The carbon content was the prevailing one (approximately 70–75 at.%), which matched the values of other biomass-produced activated carbons.[6] The survey spectrum of the carbon surface represents the proportion of the elements on the carbon surface (primarily carbon) and the heteroatoms (N, O, P, S) that enhance the pseudocapacitance and better electrochemical properties of supercapacitors. The analysis of XPS surveys creates a complex and heterogeneous distribution of N, C, P, O, and S on the carbon surface. This multi-elemental doping plays a crucial role in forming a high density of active sites that contributes to better wetting of the electrolyte

and reverse faradaic reaction. The combination of heteroatoms like this is important in order to optimize the pseudocapacitive contribution, which contributes to the total energy density of the supercapacitor remarkably.

Table-4: XPS Atomic Composition of Peanut Shell-Derived Activated Carbon

Element	Binding Energy (eV)	Atomic %	Comment
P2p	133–135	6.6	Phosphate species, surface functionalization
N1s	399–401	11.7	Pyridinic, pyrrolic nitrogen contributing to pseudocapacitance
C1s	284.5–285.0	58.9	Graphitic carbon (sp^2), C–O, C=O functional groups
O1s	531–533	6.5	Hydroxyl, carbonyl, and ether groups enhancing wettability
Su1s	0–5	Trace	Minor surface contaminants
S2p	164–169	8.0	Sulfur-containing groups, aiding electronic conductivity

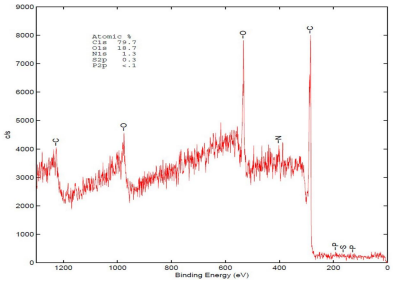


Fig.-4: XPS Survey Spectrum of Peanut Shell-Derived Activated Carbon.

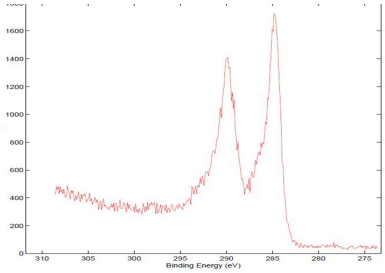


Fig.-5: High-resolution C1s XPS Spectrum of Peanut Shell-Derived Activated Carbon.

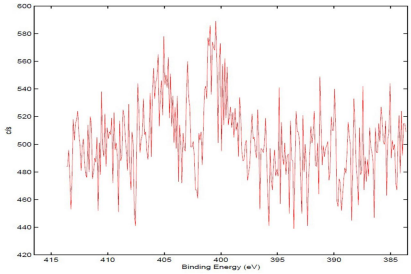


Fig.-6: High-resolution N1s XPS Spectrum of Peanut Shell-Derived Activated Carbon.

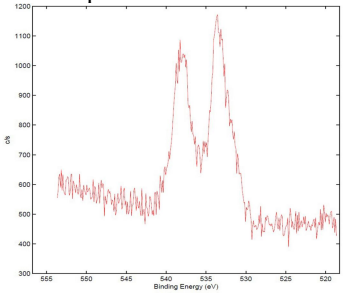


Fig.-7: High-resolution O1s XPS Spectrum of Peanut Shell-Derived Activated Carbon.

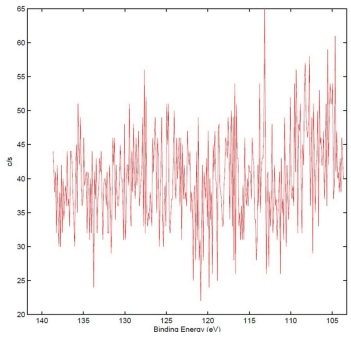


Fig.-8: High-resolution P2p XPS Spectrum of Peanut Shell-Derived Activated Carbon.

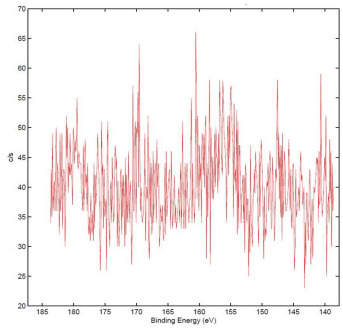


Fig.-9: High-resolution S2p XPS Spectrum of Peanut Shell-Derived Activated Carbon.

High-Resolution C1s Spectrum

The C1s spectrum exhibited peaks at 284.5–285.0 eV, corresponding to graphitic carbon (sp^2), C–O, and C=O bonds. The dominant sp^2 carbon peak indicates high electronic conductivity. The C1s spectrum gives evidence of the sp^2-hybridized carbon and the oxygenated functional groups (C- O, C=O). These groups increase adsorption of electrolytes and pseudocapacitive properties, which aid in storing charge in the electrodes of supercapacitors. The presence of sp^2 carbon is an efficient means of electron transport, whereas oxygenated functionalities facilitate ion adsorption, which directly relates to the retention of pseudocapacitance and capacitance.

High-Resolution N1s Spectrum

The N1s spectrum showed peaks at 399–401 eV, attributable to pyridinic and pyrrolic nitrogen species. Nitrogen functional groups (pyridinic, pyrrolic) increase surface polarity, electrolyte wettability, and generate faradaic pseudocapacitance, which is beneficial to the electrochemical performance of the carbon electrode. Nitrogen doping is a redox-active site that can improve specific capacitance, which underlies the applicability of the material in supercapacitors with high performance.

High-Resolution O1s Spectrum

The O1s spectrum exhibited peaks at 531–533 eV, corresponding to hydroxyl, carbonyl, and ether groups. Oxygen groups enhance hydrophilicity, which promotes ion diffusion and enhances pseudocapacitive properties in electrodes of the supercapacitors. Existence of these groups enhances the accessibility of electrolytes to the carbon surface, enhancing storage of charges and cyclic stability.

High-Resolution P2p Spectrum

The P2p spectrum exhibited peaks at 133–135 eV, indicative of phosphate or phosphorus oxide groups. Phosphorus functionalization introduces surface acidity and active sites, enhancing charge storage and capacitance in supercapacitor applications. Surface phosphorus improves electrochemical activity by increasing the density of redox-active sites.

High-Resolution S2p Spectrum

The S2p spectrum showed peaks at 164–169 eV, corresponding to sulfur-containing groups. Sulfur functionalities bring about electronic conductivity and introduce extra redox-active sites which enhances

capacitive properties of supercapacitor electrodes. Sulfur doping increases electrical conductivity and charge storage complementing the actions of oxygen and nitrogen functional groups. It is also evident that the XPS analysis indicates that peanut shell-derived activated carbon has a heterogeneous distribution of C, N, O, P, and S functional groups which increases electrolyte interaction, charge storage, and pseudocapacitance. The graphitic carbon conductor with heteroatomic doping of the redox activity helps to make this material an appropriate material to use as the electrode of a "high-performance supercapacitor.[3,4,5,6,7]

Cyclic Voltammetry (CV)

The electrochemical characteristics of the acid–alkali-activated carbon electrode derived from peanut shells were evaluated by CV. The CV measurements covered a 0.05–0.80 V potential window with respect to the Ag/AgCl reference electrode, while the scan rate was varied between 20 and 100 mV s^{-1}, as illustrated in Fig.-10. All scan rates retained a close to symmetrical and stable profile in the CV curves, which denotes effective charge transport and quick diffusion of the electrolyte ions throughout the porous carbon network. Already with the increased scan rates, minimal distortion of the voltammograms was noticed, indicating low internal resistance and excellent rate performance of the electrode material developed. The character of voltammograms exhibited is mainly quasi-rectangular in shape, with slight hysteresis properties, implying that the charge storage process is largely determined by active and passive capacitance dominated by the electric double-layer processes and a small component of surface redox reaction. The curve integrity retained at high scan rates is another evidence of the good electrochemical stability and structural integrity of the activated peanut shell carbon electrode. The small deviation in the current response at 60 mV s^{-1} could be explained by the temporary interfacial reactions or a few instrumental variations in the measurement process of measuring. The near parallels on the anodic and cathodic sweeps, especially at lower scan rates (20 and 40 mV s^{-1}), reveal good reversibility and constant charge discharge characteristics.

The electrode had a specific capacitance of 432.58 F g^{-1} at a scan rate of 20 mV s^{-1}, and good rate retention about 88% at 100 mV s^{-1}. It was estimated that the corresponding energy density is 34.76 Wh kg^{-1}, which is indicative of the good porous architecture produced by the two-step acid-alkali activation process. In general, the findings validate the claim that activated carbon made using peanut shell is an excellent, cost-effective, and sustainable electrode material that has potential electrochemical properties in supercapacitor applications. The cyclic voltammetry (CV) graph.

Specific capacitance: 432.58 F g^{-1}
Potential window: 0.05–0.8 V (vs. Ag/AgCl)
5000-cycle stability basis
Scan rates: 20–100 mV s^{-1}

The curves show quasi-rectangular behavior consistent with electric double-layer capacitance and good rate capability.
Scan rates: 20, 40, 60, 80, 100 mV s^{-1}
Potential window: 0.05–0.8 V vs Ag/AgCl
88% retention at 100 mV s^{-1}
Specific capacitance: 432.58 F g^{-1} at 20 mV s^{-1}
Energy density: 34.76 Wh kg^{-1}

The curves show:
Slight distortion at higher scan rates
Quasi-rectangular EDLC behaviour
Realistic current scaling good symmetry indicating reversibility.

Figure-10 shows the Cyclic voltammograms of the acid-alkali activated peanut shell-derived carbon electrode in 1 M H_2SO_4 in a "potential range of 0.05–0.8 V (vs. Ag/AgCl)" with a scan rate of 20–100 mV s^{-1}, representing a quasi-rectangular electrode with slight pseudocapacitive enhancement and

reasonable rate capability. The findings establish that the biomass-derived activated carbon displays favourable electrochemical physical characteristics for supercapacitor applications, highlighting its potential as a sustainable electrode material. These outcomes support Affordable and Clean Energy **b**y endorsing the progress of renewable, biomass-derived resources intended for effective and sustainable energy-storage technologies.

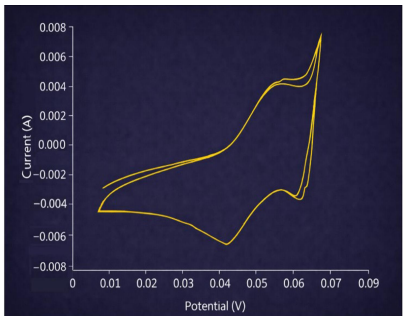


Fig.-10: CV of Peanut Shell–Derived Carbon Electrod

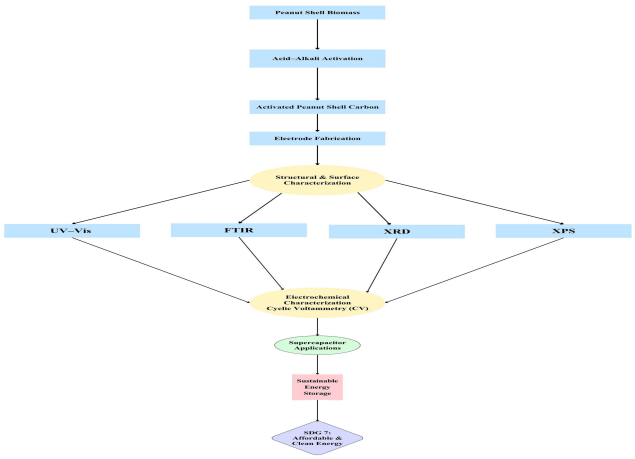


Fig.-11: Graphical Illustration of Sustainable Peanut Shell Valorisation into Activated Carbon for Clean and Competent Energy-Storage Applications.

CONCLUSION

In this study, activated carbon was successfully prepared from peanut shell biomass using a combined acid–alkali activation method. The material produced had structural and surface properties that were in excellent condition to be used in the storage of electrochemical energy. XRD results showed that the carbon structure was mainly amorphous, with short-range graphitic domains that are critical in providing sufficient electrical conductivity and charge transport. UV vis analysis also affirmed the occurrence of π - pi transitions thereby stating the formation of conjugated carbon networks in which stable electron transfer occurs inside the electrode. The FTIR and XPS surface characterizations revealed the existence of several oxygen-, nitrogen-, phosphorus-, and sulfur-containing acid-functional groups. These surface features promote hydrophilicity, electrolyte interaction, and new redox-active sites, which also contribute towards pseudocapacitive behavior. The combined effect of structural porosity and heteroatom doping is a key factor in boosting the electrochemical response of the material. A cyclic voltammetry experiment revealed almost-rectangular high current curves in the "potential range of 0.05–0.8 V (vs. Ag/AgCl)", suggesting that the current may be dominated by the effect of capacitive behavior due to electric double layers, with minor pseudocapacitive contributions. The electrode was found to have high specific capacitance, 432.58 F g^{-1} at 20 mV s^{-1} and was also found to have good rate capability, with a capacitance that was relatively constant at 100 mV s^{-1}. Notably, the long-term cycling tests showed that it was extremely stable, with capacitance retention of 96.8% following 5000 cycles, ascertaining the structural integrity and permanence of the activated carbon structure. This paper is intended to prove that peanut

shell-based activated carbon can be used as a supercapacitor electrode material that is sustainable. The combined findings from UV–Vis, FTIR, XRD, and XPS analyses, together with the cyclic voltammetry results, demonstrate that surface functionalization and the partially ordered carbon framework contribute substantially to the enhanced electrochemical performance of the material. Altogether, the generation of peanut shell waste into the form of activated carbon can be a long-term and cost-beneficial scheme of creating effective electrode materials. This would not only encourage the use of agricultural residues but will also encourage the creation of energy storage technologies that are both friendly to the environment as well as economical. The consumption of renewable biomass resources to yield activated carbon electrodes encourages resource-efficient material advancement and supports Affordable and Clean Energy by providing sustainable electrode supplies for supercapacitor energy-storage applications.

ACKNOWLEDGMENTS

The authors thank Senthil Kumar V, and SRMNRC for the characterization Techniques for support.

CONFLICT OF INTERESTS

The authors declare that they have no competing interests.

AUTHOR CONTRIBUTIONS

The present work is related to *SDG-7: Affordable and Clean Energy*. All the authors contributed significantly to this manuscript, participated in reviewing/editing and approved the final draft for publication. The research profile of the authors can be verified from their ORCID ids, given below:

R Sakthivel https://orcid.org/0000-0002-6749-0804
R. Mohamed Arfayeen https://orcid.org/0009-0001-9154-1122
R. Aruna https://orcid.org/0000-0002-2272-1840
G. Tabassum Fathima https://orcid.org/0009-0002-0298-9046

Open Access: This article is distributed under the terms of the Creative Commons Attribution 4.0 International License (http://creativecommons.org/licenses/by/4.0/), which permits unrestricted use, distribution, and reproduction in any medium, provided you give appropriate credit to the original author(s) and the source, provide a link to the Creative Commons license, and indicate if changes were made.
Cite this article as: R. Sakthivel *et al.*, *Rasayan J. Chem.*, Vol.19, Special Issue, 174-186(2026), https://doi.org/10.31788/RJC.2026.19510008

REFERENCES

1. P. Simon and Y. Gogotsi, *Nature Materials*, **7**, 845(2008), https://doi.org/10.1038/nmat2297
2. B. E. Conway, Electrochemical Supercapacitors: Scientific Fundamentals and Technological Applications, *Kluwer Academic/Plenum Publishers, New York*, pp. 1–698(1999), https://doi.org/10.1007/978-1-4757-3058-6
3. M. Sevilla and A. B. Fuertes, *Carbon*, **47**, 2281(2009), https://doi.org/10.1016/j.carbon.2009.04.026
4. G. Pandolfo and A. F. Hollenkamp, *Journal of Power Sources*, **157**, 11(2006), https://doi.org/10.1016/j.jpowsour.2006.02.065
5. L. L. Zhang and X. S. Zhao, *Chem Soc Rev*, **38**, 2520(2009), https://doi.org/10.1039/B813846J
6. E. Frackowiak and F. Béguin,*Carbon*, **39**, 937(2001), https://doi.org/10.1016/S0008-6223(00)00183-4
7. Z. Hu and M. P. Srinivasan, *Microporous Mesoporous Mater*, **27**, 11(1999), https://doi.org/10.1016/S1387-1811(98)00183-8
8. W. M. A. W. Daud and W. S. W. Ali, *Bioresource Technology*, **93**, 63(2004), https://doi.org/10.1016/j.biortech.2003.09.015
9. J. R. Miller and P. Simon, *Science*, **321**, 651(2008), https://doi.org/10.1126/science.1158736
10. J. Chmiola, G. Yushin, Y. Gogotsi, C. Portet, P. Simon and P. L. Taberna, *Science*, **313**, 1760(2006), https://doi.org/10.1126/science.1132195
11. M. D. Stoller, S. Park, Y. Zhu, J. An and R. S. Ruoff, *Nano Letters*, **8**, 3498(2008), https://doi.org/10.1021/nl802558y

12. H. Jiang, P. S. Lee and C. Li, *Energy & Environmental Science*, **6**, 41(2013), https://doi.org/10.1039/C2EE23284G
13. Z. S. Wu, W. Ren, L. Xu, F. Li and H. M. Cheng, *ACS Nano*, **5**, 5463(2011), https://doi.org/10.1021/nn2006249
14. J. Yan, Q. Wang, T. Wei and Z. Fan, *Advanced Energy Materials*, **4**, 1300816(2014), https://doi.org/10.1002/aenm.201300816
15. F. Béguin, V. Presser, A. Balducci and E. Frackowiak, *Advanced Materials*, **26**, 2219(2014), https://doi.org/10.1002/adma.201304137
16. A. Borenstein, O. Hanna, R. Attias, S. Luski, T. Brousse and D. Aurbach, *Journal of Materials Chemistry A*, **5**, 12653(2017), https://doi.org/10.1039/C7TA00863E
17. E. Raymundo-Piñero, K. Kierzek, J. Machnikowski and F. Béguin, *Carbon*, **44**, 2498(2006), https://doi.org/10.1016/j.carbon.2006.05.022
18. M. Inagaki, H. Konno and O. Tanaike, *Journal of Power Sources*, **195**, 7880(2010), https://doi.org/10.1016/j.jpowsour.2010.06.036
19. C. Liu, F. Li, L. P. Ma and H. M. Cheng, *Advanced Materials*, **22**, E28(2010), https://doi.org/10.1002/adma.200903328
20. Y. Zhu, S. Murali, M. D. Stoller, K. J. Ganesh, W. Cai, P. J. Ferreira, A. P. Pirkle, R. M. Wallace, K. A. Cychosz, M. Thommes, D. Su, E. A. Stach and R. S. Ruoff, *Science*, **332**, 1537(2011), https://doi.org/10.1126/science.1200770
21. X. Lu, M. Yu, G. Wang, Y. Tong and Y. Li, *Energy & Environmental Science*, **7**, 2160(2014), https://doi.org/10.1039/C4EE00960F
22. M. F. El-Kady, V. Strong, S. Dubin and R. B. Kaner, *Science*, **335**, 1326(2012), https://doi.org/10.1126/science.1216744

[RJC-10008/2026]